

# Study of the Reactions of Fullerene C<sub>60</sub> with the Palladium-Containing Clusters of Molybdenum {Mo<sub>3</sub>PdS<sub>4</sub>} by Spectroscopic and Calculation Methods

Yu. A. Laricheva<sup>a</sup>, N. Yu. Shmelev<sup>a, b</sup>, A. L. Gushchin<sup>a, \*</sup>, and M. N. Sokolov<sup>a, c</sup>

<sup>a</sup> Nikolaev Institute of Inorganic Chemistry, Siberian Branch, Russian Academy of Sciences, Novosibirsk, 630090 Russia

<sup>b</sup> Novosibirsk State University, Novosibirsk, 630090 Russia

<sup>c</sup> Kazan Federal University, Kazan, Russia

\*e-mail: gushchin@niic.nsc.ru

Received July 24, 2020; revised August 27, 2020; accepted September 1, 2020

**Abstract**—The fabrication of hybrid materials combining the physicochemical properties of various classes is a complicated but promising trend for the development of the modern science. The formation of new hybrid cluster cations [Mo<sub>3</sub>Pd(C<sub>60</sub>)S<sub>4</sub>Cl<sub>3</sub>(R<sub>2</sub>Bipy)<sub>3</sub>]<sup>+</sup> and [{Mo<sub>3</sub>PdS<sub>4</sub>Cl<sub>3</sub>(R<sub>2</sub>Bipy)<sub>3</sub>}<sub>2</sub>(C<sub>60</sub>)]<sup>2+</sup> (Bipy is 2,2-bipyridine) containing fullerene C<sub>60</sub> coordinated to the palladium atom by the reaction of [Mo<sub>3</sub>S<sub>4</sub>Cl<sub>3</sub>(R<sub>2</sub>Bipy)<sub>3</sub>]PF<sub>6</sub> with Pd<sub>2</sub>(Dba)<sub>3</sub> (Dba is dibenzylideneacetone) and C<sub>60</sub> is shown by a complex of physicochemical methods. The reaction products are studied by IR and NMR (<sup>1</sup>H, <sup>31</sup>P, and C–H correlations) spectroscopy and mass spectrometry. The quantum-chemical calculations are performed by the DFT method for the correct interpretation of the spectroscopic data and elucidation of the electronic structures of the fullerene-containing compounds.

**Keywords:** molybdenum, palladium, fullerene, cluster complexes, DFT calculations

**DOI:** 10.1134/S1070328421020032

## INTRODUCTION

Since the methods for the synthesis of fullerenes have been developed, these compounds became objects of numerous studies due to the unique structures and corresponding physicochemical properties [1]. “Fullerene par excellence” C<sub>60</sub> is the most available and abundant fullerene. The term “fullerene” further implies the C<sub>60</sub> molecule. The spatial structure of this molecule and specific features of the electronic structure (Fig. 1, at the right), such as the fivefold degeneration of the highest occupied molecular orbital (HOMO) low-lying in energy (h<sub>u</sub>), threefold degeneration of the lowest unoccupied molecular orbital (LUMO) (t<sub>lu</sub>), and a relatively low discrepancy between the frontier orbitals (~1.6 eV), are reasons for the attractive properties of fullerene and related compounds: the redox [2–4], catalytic [5–7], optical [8], photovoltaic [9], and magnetic [10] properties, as well as toxicity [11], antimicrobial activity [12], and others [13–16].

There are four main types of reactions affording transition metal complexes with fullerenes [16]. The first type includes the coordination of the metal at the bond between the six-membered rings (6–6) (Fig. 1, at the left), which is olefinic in character, to form  $\eta^2$ -coordination complexes. The second type of the reac-

tion is the reduction of fullerene to form a fulleride salt. The third type is the functionalization of fullerene by the “bridging” groups to which the metal is coordinated. The fourth type is the formation of cocrystallizates of fullerene and metal complex and can include some degree of charge transfer between particular components.

For the  $\eta^2$  coordination of fullerene to palladium(0), the backward donation of the electron density from the *d* orbitals of the metal to the  $\pi^*$  orbitals of fullerene predominates over the  $\sigma$  donation. Fullerene by the acceptor ability occupies an intermediate position between ethylene and electron-deficient alkenes: tetracyanoethylene and tetrafluoroethylene. The low oxidation state of Pd(0) and the strong  $\pi$ -acceptor nature of C<sub>60</sub> lead to a strong Pd–fullerene coupling. The calculated dissociation energies of the Pd–C bond are higher than those for the corresponding complexes with ethylene but are lower than those for complexes with the strong acceptors: tetracyanoethylene or tetrafluoroethylene [17].

Many heterometallic cubane complexes {M<sub>3</sub>M'S<sub>4</sub>}<sup>n+</sup> were described [18–24]. They are formed most frequently in the reactions of the trinuclear molybdenum or tungsten clusters {M<sub>3</sub>S<sub>4</sub>} with com-

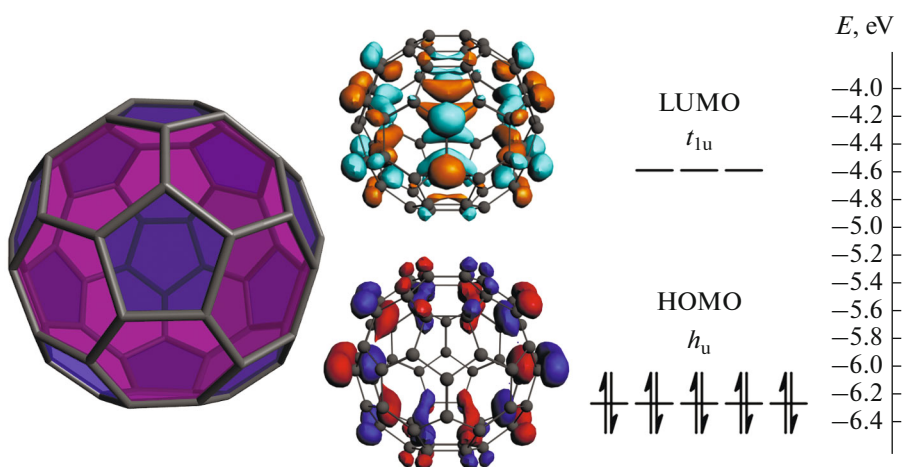


**Fig. 1.** Molecular structure of fullerene C<sub>60</sub> (at the left): six-membered rings are violet-colored, five-membered rings are blue-colored; and the view of the frontier orbitals and energy levels for fullerene C<sub>60</sub> (at the right).

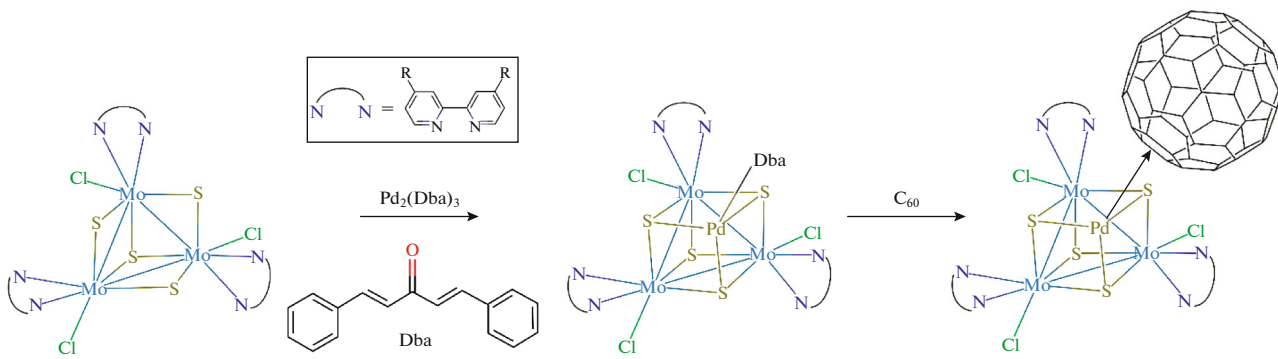


**Fig. 2.** Scheme of the [3 + 1] formation of the palladium-containing cubane complexes with the bipyridine ligands (R = <sup>11</sup>C<sub>9</sub>H<sub>19</sub>, <sup>1</sup>Bu).

plexes of various transition metals M' in low oxidation states (0–II) (Fig. 2).

Such heterometallic clusters often demonstrate a high catalytic activity in diverse reactions of organic synthesis [22]. In particular, the palladium-containing clusters {M<sub>3</sub>PdS<sub>4</sub>} first described by Japanese scientists [25, 26] catalyze the allylation of aromatic compounds [27–29] and nucleophilic addition to the triple bond [25, 30] and can stabilize such forms of acids as As(OH)<sub>3</sub>, P(OH)<sub>3</sub>, PhP(OH)<sub>2</sub>, Ph<sub>2</sub>P(OH), and P(OH)<sub>2</sub>H in the coordination sphere of palladium [31, 32]. Taking into account the stability of the known mononuclear Pd complexes with fullerene and interesting properties of both fullerene and heterometallic Pd-containing clusters, we aimed at synthesizing the cluster complexes [Mo<sub>3</sub>Pd(Dba)S<sub>4</sub>Cl<sub>3</sub>(R<sub>2</sub>Bipy)<sub>3</sub>]<sup>+</sup> and at studying their reactions with fullerene C<sub>60</sub> followed by the isolation of new hybrid compounds. It was found in the studies that the coordination of fullerene occurred indeed, but the products of these reactions were always mixtures of complexes, because fullerene

contains sufficiently high number of accessible coordination sites. In spite of the applied efforts, we failed to isolate individual compounds and obtain crystals suitable for X-ray diffraction analysis. A similar behavior of complicated nonsymmetric sterically hindered fullerene compounds is an abundant problem.

## EXPERIMENTAL

The starting compounds [Mo<sub>3</sub>S<sub>4</sub>Cl<sub>3</sub>(Dbbipy)<sub>3</sub>]PF<sub>6</sub> and [Mo<sub>3</sub>S<sub>4</sub>Cl<sub>3</sub>(Dnbipy)<sub>3</sub>]PF<sub>6</sub> (Dbbipy is 4,4'-di-*tert*-butyl-2,2'-bipyridine and Dnbipy is 4,4'-di-*n*-nonyl-2,2'-bipyridine) were synthesized according to published procedures [33, 34]. Other reagents and solvents were purchased from commercial sources, and all of them were not worse than analytical grade. The solvents were purified by distillation according to standard procedures if not additionally specified. The complexes were synthesized in air or in argon (special purity grade) using the Schlenk techniques.

IR spectra were recorded in a range of 4000–400  $\text{cm}^{-1}$  in KBr pellets on Scimitar FTS 2000 and Vertex 80 Fourier spectrometers. Electrospray mass spectra were detected on Agilent (6130 Quadrupole MS, 1260 infinity LC) and Micromass Q-ToF Premier mass spectrometers. NMR spectra were recorded on Agilent 500, Agilent 600 DD2, and Bruker Avance 500 instruments using internal standards for  $^1\text{H}$  (TMS),  $^{13}\text{C}$  (TMS), and  $^{31}\text{P}$  ( $\text{H}_3\text{PO}_4$ ). Elemental analyses to C, H, N, and S were carried out on a Euro EA 3000 instrument.

The geometry optimization of the  $[\text{Mo}_3\text{Pd}(\text{C}_{60})\text{S}_4\text{Cl}_3(\text{Bipy})_3]^+$  cluster was performed in the ADF2017 program package [35] using the all-electron TZ2P basis set for all elements and VWN and BP functionals. Relativistic effects were applied by the ZORA zero-order regular approximation. No negative values were found by optimization. Using the obtained geometry, the NMR spectra were calculated in a chloroform solution for the optimized structure of  $[\text{Mo}_3\text{Pd}(\text{C}_{60})\text{S}_4\text{Cl}_3(\text{Bipy})_3]^+$  in the GAUSSIAN G16.A03 program package [36] using the B3LYP-GD3BJ/6-31+g(d,p) hybrid functional for all atoms. No negative frequencies were either observed.

**Reaction of  $[\text{Mo}_3\text{S}_4\text{Cl}_3(\text{Dbbipy})_3](\text{PF}_6)$  with  $\text{Pd}_2(\text{Dba})_3\cdot\text{CHCl}_3$  and  $\text{C}_{60}$ .** A mixture of solid substances  $\text{Pd}_2(\text{Dba})_3\cdot\text{CHCl}_3$  (0.035 g, 33.9  $\mu\text{mol}$ ),  $[\text{Mo}_3\text{S}_4\text{Cl}_3(\text{Dbbipy})_3](\text{PF}_6)$  (0.1 g, 67.8  $\mu\text{mol}$ ), and  $\text{C}_{60}$  (50 mg, 67.8  $\mu\text{mol}$ ) was dried in vacuo for 1 h and dissolved in deaerated toluene (20 mL) in an argon flow. The mixture was refluxed for 5 h. The resulting solution was evaporated on a rotary evaporator to dryness, redissolved in  $\text{CH}_2\text{Cl}_2$ , and precipitated with hexane. A black solid was obtained, washed with ether, and dried in vacuo.

For  $\text{Mo}_3\text{S}_4\text{PdCl}_3\text{C}_{114}\text{H}_{72}\text{N}_6\text{PF}_6$

Anal. calcd., %	N, 3.7	C, 59.5	H, 3.2	S, 5.6
Found, %	N, 3.7	C, 54.0	H, 3.3	S, 5.3

IR ( $\nu, \text{cm}^{-1}$ ): 3400 w.sh, 3221 (w), 3058 w, 2962 m, 2871 w, 1735 w, 1650 m, 1615 s, 1482 m, 1448 m, 1410 m, 1337 m, 1307 w, 1253 m, 1184 m, 1098 m, 1023 w, 982.7 m, 837 vs, 766 m, 735 w, 699 s, 603 w, 555 m, 534 w, 525 m, 474 w, 433 w.  $^1\text{H}$  NMR ( $\text{CD}_3\text{CN}$ , 500 MHz),  $\delta$ , ppm: 9.81 (d,  $J = 6.11$  Hz, 3H), 9.47 (d,  $J = 6.11$  Hz, 3H), 8.35 (d,  $J = 1.60$  Hz, 3H); 8.23 (d,  $J = 1.70$  Hz, 3H); 7.56 (dd,  $J = 6.11$  Hz,  $J = 2.08$  Hz, 3H), 7.40 (dd,  $J = 6.00$  Hz,  $J = 1.80$  Hz, 3H), 1.46 (s, 27H) 1.43 (s, 27H).  $^{31}\text{P}$  NMR ( $\text{CD}_3\text{CN}$ , 500 MHz),  $\delta$ , ppm: –144.27.

ESI-MS (+;  $\text{CH}_2\text{Cl}_2/\text{CH}_3\text{OH}$ ;  $m/z$ ): 2153.4  $[\text{Mo}_3\text{Pd}(\text{C}_{60})\text{S}_4\text{Cl}_3(\text{Dbbipy})_3]^+$ , 1792.6  $\{[\text{Mo}_3\text{PdS}_4\text{Cl}_3(\text{Dbbipy})_3]_2(\text{C}_{60})\}^{2+}$ , 1328.1  $[\text{Mo}_3\text{S}_4\text{Cl}_3(\text{Dbbipy})_3]^+$ , 1055.1  $[\text{Mo}_3\text{Pd}(\text{C}_{60})\text{S}_4\text{Cl}_2(\text{Dbbipy})_3]^{2+}$ .

**Reaction of  $[\text{Mo}_3\text{S}_4\text{Cl}_3(\text{Dnbipy})_3]\text{PF}_6$  with  $\text{Pd}_2(\text{Dba})_3\cdot\text{CHCl}_3$  and  $\text{C}_{60}$ .** A mixture of  $\text{Pd}_2(\text{Dba})_3\cdot\text{CHCl}_3$  (74 mg, 0.14 mmol),  $[\text{Mo}_3\text{S}_4\text{Cl}_3(\text{Dnbipy})_3]\text{PF}_6$  (400 mg, 0.28  $\mu\text{mol}$ ), and  $\text{C}_{60}$  (220 mg, 0.28 mmol) in toluene (40 mL) was refluxed in an inert atmosphere for 48 h. The further treatment procedure was similar to that used in the previous synthesis.

For  $\text{C}_{144}\text{H}_{132}\text{F}_6\text{N}_6\text{S}_4\text{PCl}_3\text{Mo}_3\text{Pd}$

Anal. calcd., %	N, 3.1	C, 63.6	H, 4.9	S, 4.7
Found, %	N, 3.0	C, 67.9	H, 4.7	S, 3.5

IR ( $\nu, \text{cm}^{-1}$ ): 2922 s, 2850 s, 1614 s, 1553 w, 1487 w, 1461 m, 1418 m, 1288 w, 1243 w, 1182 m, 1102 w, 1024 m, 912 w, 842 vs, 737 w, 704 m, 577 m, 557 m, 536 w, 526 s, 491 w, 436 w.  $^1\text{H}$  NMR ( $\text{CD}_3\text{CN}$ , 500 MHz),  $\delta$ : 9.83 s, 9.81 s, 9.8 s, 9.79 s, 9.51 s, 9.50 s, 9.49 (d,  $J = 3.18$  Hz), 9.46 s, 9.45 s, 9.38 s, 9.37 s, 8.36 s, 8.35 s, 8.31 s, 8.30 s, 8.25 s, 8.24 s, 8.20 s, 8.16 (d,  $J = 1.59$  Hz), 8.10 (d,  $J = 1.83$  Hz), 7.56 (d,  $J = 1.71$  Hz), 7.55 (d,  $J = 1.71$  Hz), 7.46 (d,  $J = 1.96$  Hz), 7.44 (d,  $J = 1.96$  Hz), 7.43 (d,  $J = 1.96$  Hz), 7.41 (d,  $J = 1.71$  Hz), 7.40 (d,  $J = 2.20$  Hz), 7.38 (d,  $J = 1.83$  Hz), 1.88 (dd,  $J = 7.21$  Hz,  $J = 7.34$  Hz), 1.72 m, 1.62 m, 1.52 m, 1.46 m, 1.45 s, 1.43 s, 1.42 s, 1.40 s, 1.37 s, 1.30 s, 1.27 s.  $^{13}\text{C}$  NMR ( $\text{CD}_3\text{CN}$ , 500 MHz),  $\delta$ : 13.85 and 13.92 (s,  $\text{CH}_3$ ), 22.65 and 22.72 (s,  $\text{CH}_2$ ), 29.39 (m,  $\text{CH}_2$ ), 31.85 and 31.92 (s,  $\text{CH}_2$ ), 35.58 and 35.64 (s,  $\text{CH}_2$ ), 122.79–126.72 (s, Bipy), 141.90 and 143.00 (s,  $\text{C}_{60}$ ), 153.01–157.76 (s, Bipy,  $\text{C}_{60}$ ). ESI-MS (+;  $\text{CH}_2\text{Cl}_2/\text{CH}_3\text{OH}$ ):  $m/z = 2575.4$   $[\text{Mo}_3\text{Pd}(-\text{C}_{60})\text{S}_4\text{Cl}_3(\text{Dnbipy})_3]^+$ , 2215.8  $\{[\text{Mo}_3\text{PdS}_4\text{Cl}_3-(\text{Dnbipy})_3]_2(\text{C}_{60})\}^{2+}$ , 1855.3  $[\text{Mo}_3\text{PdS}_4\text{Cl}_3-(\text{Dnbipy})_3]^+$ , 1748.4  $[\text{Mo}_3\text{S}_4\text{Cl}_3(\text{Dnbipy})_3]^+$ .

## RESULTS AND DISCUSSION

In this work, we studied a possibility of the coordination of  $\text{C}_{60}$  to palladium in the  $[\text{Mo}_3\text{Pd}-(\text{Dba})\text{S}_4\text{Cl}_3(\text{R}_2\text{Bipy})_3]^+$  cubane complexes synthesized *in situ* without isolation and characterization (Fig. 2). We have previously described the formation of a similar cubane complex  $[\text{Mo}_3\text{Pd}(\text{Tu})-\text{S}_4\text{Cl}_3(\text{Dbbipy})_3]\text{Cl}$  in which the coordination site at palladium is occupied by a thiourea (Tu) molecule [37]. The cubane complexes  $[(\text{Cp}^*\text{M})_3\text{S}_4\text{Pd}-(\text{Dba})]\text{PF}_6$  ( $\text{M} = \text{Mo, W}$ ) containing the  $\text{Pd}(\text{Dba})$  fragment are also known, and their properties were described [28, 29, 38].

The reactions were carried out under the conditions resembling those for the synthesis of  $[\text{Mo}_3\text{Pd}(\text{Tu})\text{S}_4\text{Cl}_3(\text{Dbbipy})_3]\text{Cl}$  with the only exception that toluene was used as the solvent because of the low solubility of fullerene in chlorinated hydrocarbons and acetonitrile. Thus, solutions of complexes

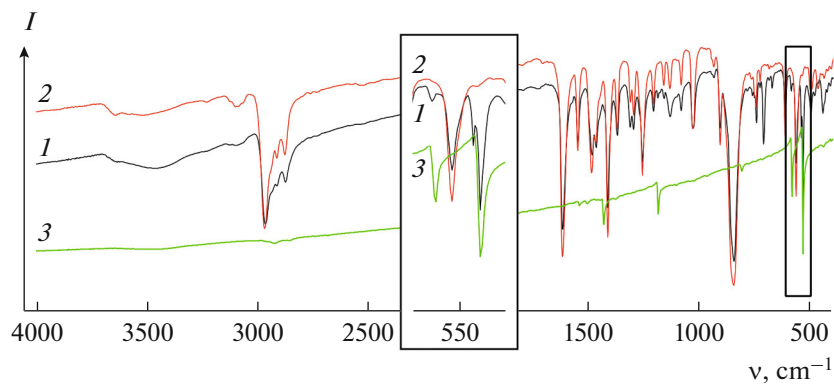


**Fig. 3.** Comparison of the IR spectra of (1) [Mo<sub>3</sub>S<sub>4</sub>Cl<sub>3</sub>(Dnbipy)<sub>3</sub>]PF<sub>6</sub>, (2) product of the reaction with Pd<sub>2</sub>(Dba)<sub>3</sub>·CHCl<sub>3</sub> and C<sub>60</sub>, and initial fullerene (3).

[Mo<sub>3</sub>S<sub>4</sub>Cl<sub>3</sub>-(Dnbipy)<sub>3</sub>]PF<sub>6</sub> or [Mo<sub>3</sub>S<sub>4</sub>Cl<sub>3</sub>(Dnbipy)<sub>3</sub>]PF<sub>6</sub> with the stoichiometric amounts of Pd<sub>2</sub>(Dba)<sub>3</sub>·CHCl<sub>3</sub> and C<sub>60</sub> in toluene were added to the reaction mixture. In both cases, reflux of the reaction mixture in argon resulted in the formation of dark blue solutions. Solid products were isolated as a black powder after hexane was layered onto the solutions in methylene dichloride. However, no crystals suitable for X-ray diffraction analysis were obtained. Therefore, a complex of physicochemical methods of analysis was used to identify the synthesized compounds.

It is known from published data that the coordination of fullerene to the metal center is accompanied by the characteristic splitting of the intense band at  $\sim 510$  cm<sup>-1</sup>, which is observed in the IR spectrum of pure fullerene C<sub>60</sub> along with the bands at 1400, 1180, and 580 cm<sup>-1</sup>. The splitting of the band at 510 cm<sup>-1</sup> to 534 and 525 and 536 and 526 cm<sup>-1</sup> was observed in the IR spectra recorded for the reaction products of fullerene with [Mo<sub>3</sub>S<sub>4</sub>Cl<sub>3</sub>(Dnbipy)<sub>3</sub>]<sup>+</sup> and [Mo<sub>3</sub>S<sub>4</sub>Cl<sub>3</sub>-(Dbbipy)<sub>3</sub>]<sup>+</sup>, respectively (Fig. 3). The characteristic splitting allows one to conclude about the occurred coordination of fullerene.

The elemental analysis data to C, H, N, and S showed a substantial divergence for carbon for both products together with a satisfactory agreement for other elements. The values obtained are by 3–4% lower than those calculated for the formula [Mo<sub>3</sub>Pd(C<sub>60</sub>)S<sub>4</sub>Cl<sub>3</sub>(R<sub>2</sub>Bipy)<sub>3</sub>]PF<sub>6</sub>, which could be caused by a “deficient” of fullerene C<sub>60</sub> with respect to the cluster. The results of the NMR and mass spectra confirmed this assumption and showed that the reaction of [Mo<sub>3</sub>S<sub>4</sub>Cl<sub>3</sub>(Dbbipy)<sub>3</sub>]PF<sub>6</sub> or [Mo<sub>3</sub>S<sub>4</sub>Cl<sub>3</sub>-(Dnbipy)<sub>3</sub>]PF<sub>6</sub> with Pd<sub>2</sub>(Dba)<sub>3</sub>·CHCl<sub>3</sub> and C<sub>60</sub> afforded a mixture of products.

The electrospray mass spectra contain the signal from the single-charge particle [Mo<sub>3</sub>Pd-(C<sub>60</sub>)S<sub>4</sub>Cl<sub>3</sub>(L)<sub>3</sub>]<sup>+</sup> (*m/z*: 2575.4 for L = Dnbipy and 2153.4 for L = Dbbipy) and also the signal from the

product of coordination of one fullerene molecule to two clusters {Mo<sub>3</sub>PdS<sub>4</sub>} and {[Mo<sub>3</sub>PdS<sub>4</sub>Cl<sub>3</sub>(L)<sub>3</sub>]<sub>2</sub>(C<sub>60</sub>)<sub>2</sub>}<sup>2+</sup> (*m/z*: 2215.8 for L = Dnbipy and 1792.6 for L = Dbbipy) (Fig. 4). The ability of fullerene to act as a polytopic ligand and form neutral, amorphous, and stable in air substances (C<sub>60</sub>)Pd<sub>n</sub> (*n* = 1–7) is well known [39]. The mass spectra also exhibit signals corresponding to the single-charge cations [Mo<sub>3</sub>PdS<sub>4</sub>Cl<sub>3</sub>(L)<sub>3</sub>]<sup>+</sup> and [Mo<sub>3</sub>S<sub>4</sub>Cl<sub>3</sub>(L)<sub>3</sub>]<sup>+</sup>, the formation of which can be related to the fragmentation of [Mo<sub>3</sub>Pd(C<sub>60</sub>)S<sub>4</sub>Cl<sub>3</sub>(L)<sub>3</sub>]<sup>+</sup> under the experimental conditions. In addition, the single-charge cations [Mo<sub>3</sub>S<sub>4</sub>Cl<sub>2</sub>(OH)(L)<sub>3</sub>]<sup>+</sup> and [Mo<sub>3</sub>S<sub>4</sub>Cl(OH)<sub>2</sub>(L)<sub>3</sub>]<sup>+</sup> are observed due to the substitution of chlorine by the hydroxy group, which is typical of the mass spectra of the clusters of this type [40, 41].

With allowance for the symmetry, the addition of palladium of the second cluster moiety to fullerene can proceed via eight various types (Fig. 5, inset). Since the cluster moiety {Mo<sub>3</sub>PdS<sub>4</sub>Cl<sub>3</sub>(Bipy)<sub>3</sub>} is fairly bulky, we assume that the insertion of palladium at two  $\eta^2$  bonds arranged in the C<sub>60</sub> molecule opposite to each other is sterically less hindered (Fig. 5, type 1).

We attempted to separate the formed mixture of products by column chromatography. For this purpose, a solid mixture of products was dissolved in CH<sub>2</sub>Cl<sub>2</sub>, introduced in a chromatographic column with silica gel (40/100), washed with CH<sub>2</sub>Cl<sub>2</sub> and acetone, and eluted with CH<sub>3</sub>CN. The resulting solutions were evaporated to dryness on a rotary evaporator and again dissolved in CH<sub>2</sub>Cl<sub>2</sub>. Hexane excess was layered onto the solutions to obtain black solid products, which were washed with ether and dried. However, in spite of all efforts applied, the procedure did not allow us to obtain individual compounds. On the contrary, according to the spectroscopic data, these manipulations instead of purification result in the decomposition of the formed products and/or formation of insoluble compounds poorly prone to analysis. Thus, no

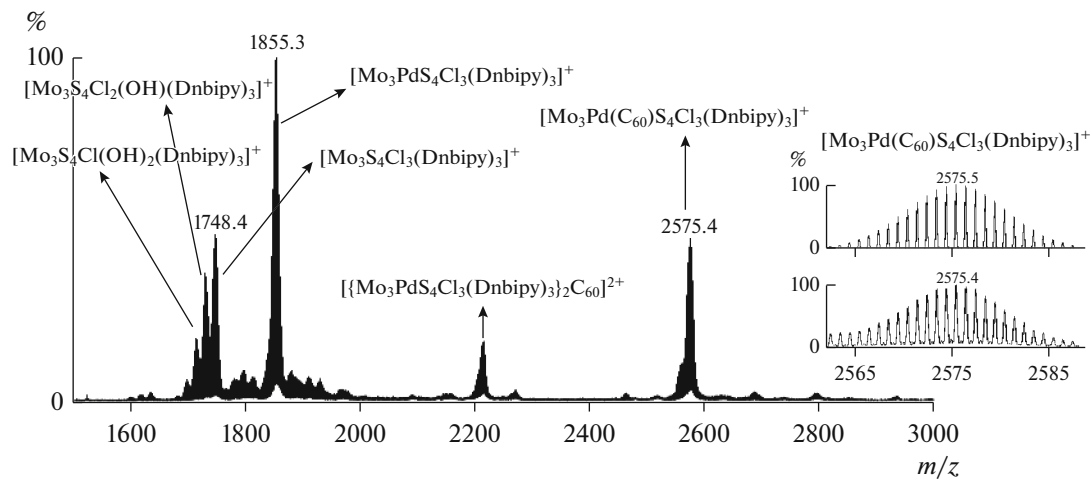


**Fig. 4.** Electrospray mass spectrum of the reaction products of  $[\text{Mo}_3\text{S}_4\text{Cl}_3(\text{Dnbipy})_3]\text{PF}_6$ ,  $\text{Pd}_2(\text{Dba})_3 \cdot \text{CHCl}_3$  and  $\text{C}_{60}$ .

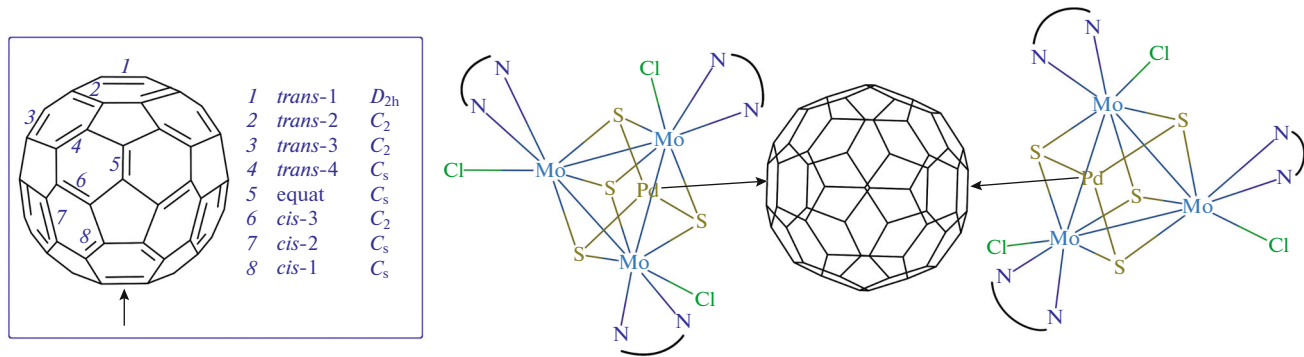


**Fig. 5.** Assumed structure of the  $\{[\text{Mo}_3\text{PdS}_4\text{Cl}_3(\text{Bipy})_3]_2(\text{C}_{60})\}^{2+}$  complex and possible symmetrically nonequivalent routes for the addition of the second metal to fullerene.

individual products of fullerene coordination to the palladium-containing clusters were isolated, but the fact of coordination was proved by different methods.

The DFT quantum-chemical calculations were performed for the additional confirmation of our interpretation of the obtained experimental data and analysis of the electronic structures. All calculations were performed for the  $[\text{Mo}_3\text{Pd}(\text{C}_{60})\text{S}_4\text{Cl}_3(\text{Bipy})_3]^+$  complex in which the hydrocarbon substituents at the bipyridine ligands were replaced by hydrogen atoms. The bond lengths calculated for the optimized geometry of  $[\text{Mo}_3\text{Pd}(\text{C}_{60})\text{S}_4\text{Cl}_3(\text{Bipy})_3]^+$  are consistent with the known crystallographic data for the palladium complexes with fullerene and the palladium-containing cubane clusters (Table 1). The coordination of fullerene via the  $\eta^2$  mode results in the elongation of the C–C bond in the corresponding 6:6 fragments, which is consistent with the literature data [17]. The bond length in the optimized fragment is 1.456 Å compared to the average value for other conjugated 6:6 fragments (1.397 Å). The Pd–C bond lengths in the

optimized structure are 2.227 and 2.210 Å. The difference in Pd–C bond lengths is typical of the palladium complexes with  $\text{C}_{60}$  usually ranging from 0.05 to 0.2 Å, depending on the nature of other ligands at palladium [13]. The geometry of the coordination mode  $\{\text{PdS}_3(\eta^2\text{-C}_2)\}$  is a distorted trigonal bipyramidal (Fig. 6) in which palladium has an environment of three  $\mu_3\text{-S}$  atoms of the metallocluster and two carbon atoms of the fullerene ligand.

A comparison of the optimized structure of  $[\text{Mo}_3\text{Pd}(\text{C}_{60})\text{S}_4\text{Cl}_3(\text{Bipy})_3]^+$  with the structures of the heterometallic clusters synthesized previously [37] showed that the presence of fullerene in the coordination environment of palladium led to the extension of the cluster core  $\{\text{Mo}_3\text{PdS}_4\}^{4+}$  along the axis of the idealized symmetry  $C_3$  passing through the  $\text{Mo}_3$  triangle and Pd atom. The average Mo–Mo, Mo–N, Mo–Pd, and Pd–( $\mu_3\text{-S}$ ) bond lengths also increase. The average Mo–( $\mu_3\text{-S}$ ) and Mo–Cl bonds are somewhat longer than the corresponding bonds in the crystal structure of  $[\text{Mo}_3\text{Pd}(\text{Tu})\text{S}_4\text{Cl}_3(\text{Dbbipy})_3]\text{Cl}$  but lower than

**Table 1.** Comparison of selected bond lengths in the complexes [Mo<sub>3</sub>S<sub>4</sub>Cl<sub>3</sub>(Dbbipy)<sub>3</sub>]<sup>+</sup> (crystallographic data) and [Mo<sub>3</sub>Pd(Tu)S<sub>4</sub>Cl<sub>3</sub>(Bipy)<sub>3</sub>]<sup>+</sup> (DFT optimization) with the optimized fragment [Mo<sub>3</sub>Pd(C<sub>60</sub>)S<sub>4</sub>Cl<sub>3</sub>(Bipy)<sub>3</sub>]<sup>+</sup>

Bond length, Å	[Mo <sub>3</sub> S <sub>4</sub> Cl <sub>3</sub> (Dbbipy) <sub>3</sub> ] <sup>+</sup>	[Mo <sub>3</sub> Pd(Tu)S <sub>4</sub> Cl <sub>3</sub> (Bipy) <sub>3</sub> ] <sup>+</sup>	[Mo <sub>3</sub> Pd(C <sub>60</sub> )S <sub>4</sub> Cl <sub>3</sub> (Bipy) <sub>3</sub> ] <sup>+</sup>
Mo–Mo	2.8115	2.8017	2.8375
Mo–(μ <sub>3</sub> -S)	2.3582	2.3422	2.3529
Mo–N	2.242	2.1713	2.2717
Mo–Cl	2.486	2.4219	2.4506
Mo–Pd	2.7966	2.7634	2.9478
Pd–(μ <sub>3</sub> -S)	2.375	2.3620	2.4262

those in the optimized complex [Mo<sub>3</sub>Pd(Tu)S<sub>4</sub>Cl<sub>3</sub>(Bipy)<sub>3</sub>]<sup>+</sup>.

The view of the optimized molecular structure and the nature of the frontier orbitals obtained from the calculations are presented in Fig. 7. The HOMO is completely cluster-centered ( $E = -7.051$  eV, atomic orbital composition: 52.1% Mo, 17.4% S, 14.7% Cl, and 10.6% Pd), whereas the LUMO ( $E = -5.898$  eV, atomic orbital composition: 89.4% C) consists of the orbitals of carbons of the fullerene ligand only, which is consistent with the  $\pi$ -acceptor nature of fullerene. Such an electron density distribution suggests that these hybrid compounds will combine both the properties of the {Mo<sub>3</sub>PdS<sub>4</sub>} cluster and fullerene and possess potentially interesting physicochemical properties.

It is known that the ranges in the <sup>13</sup>C NMR spectra in which the signals from the carbon atoms of fullerene and pyridine rings of the bipyridine ligands are mutually intersected. The spectrum of free fullerene exhibits one singlet signal at 143.2 ppm. The coordination of fullerene to one metal atom leads to a nonequivalence of the carbon atoms and complicates the spectrum

with the appearance of up to 20 signals in a range of 100 ppm and at 137–157 ppm [4, 43]. The <sup>13</sup>C NMR spectra of a mixture of products exhibits 10 singlet signals of various intensity in a range of 140–160 ppm, which can be interpreted as signals from fullerene and the bipyridine ligand. Therefore, the possibility of comparing the experimental and simulated spectra by quantum-chemical calculations and distinguishing specific signals assigned to carbon atoms of different fragments is of special interest. To save time and computational resources, the geometry optimized by the ADF program package was used for the calculation of the NMR spectra using Gaussian program package. In the obtained calculated spectra, the signals from the nonequivalent carbon atoms of fullerene coordinated to the cluster fall in a range of 140–155 ppm. The individual signal corresponds to each symmetrically non-equivalent carbon atom (Fig. 8). However, the ranges of signals from fullerene and bipyridine are not separated sufficiently to distinguish specific signals in the experimental spectrum using the calculated data.

It was shown in the present study that the reactions of the cluster complexes [Mo<sub>3</sub>S<sub>4</sub>Cl<sub>3</sub>(Dnbipy)<sub>3</sub>]PF<sub>6</sub> and

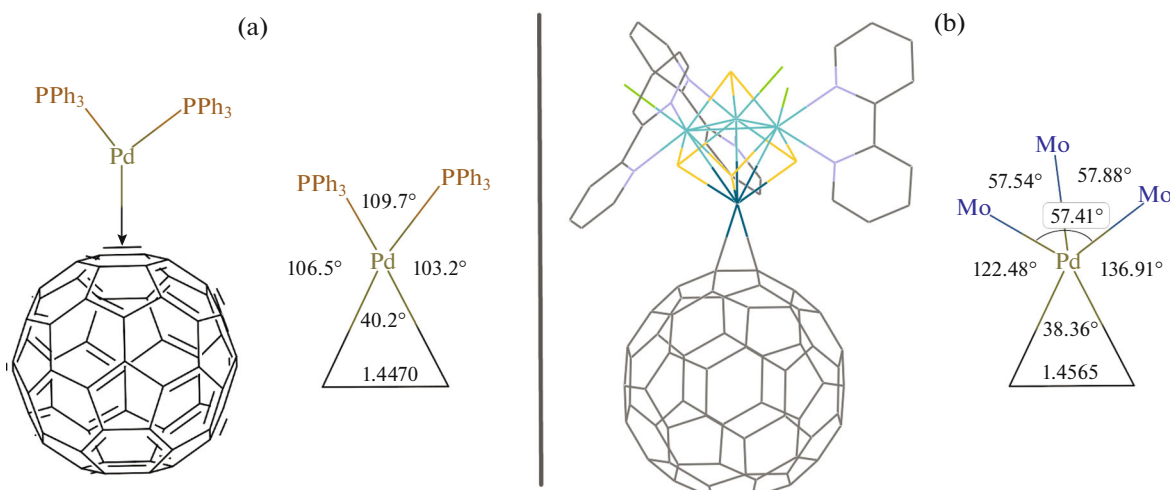


**Fig. 6.** Optimized structures and coordination environments of the Pd atom in the complexes (a) ( $\eta^2$ -C<sub>60</sub>)Pd(PPh<sub>3</sub>)<sub>2</sub> [42] and (b) [Mo<sub>3</sub>Pd(C<sub>60</sub>)S<sub>4</sub>Cl<sub>3</sub>(Bipy)<sub>3</sub>]<sup>+</sup>.

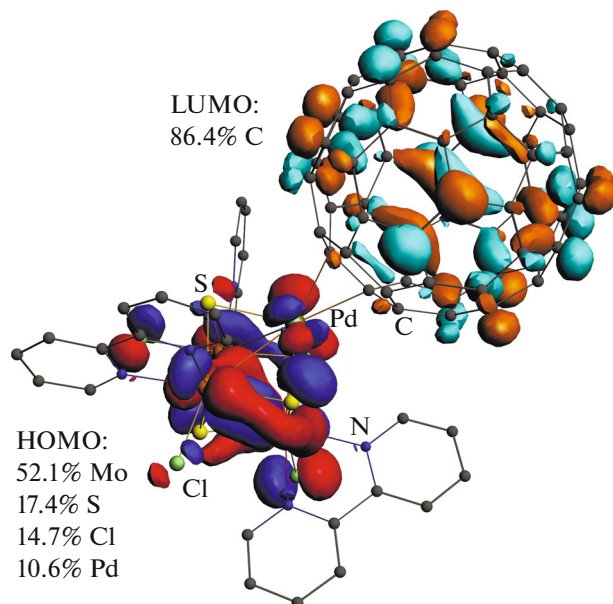


**Fig. 7.** Optimized molecular structure and the nature of the frontier orbitals of the complex  $[\text{Mo}_3\text{Pd}(\text{C}_{60})\text{S}_4\text{Cl}_3(\text{Bipy})_3]^{3+}$ .

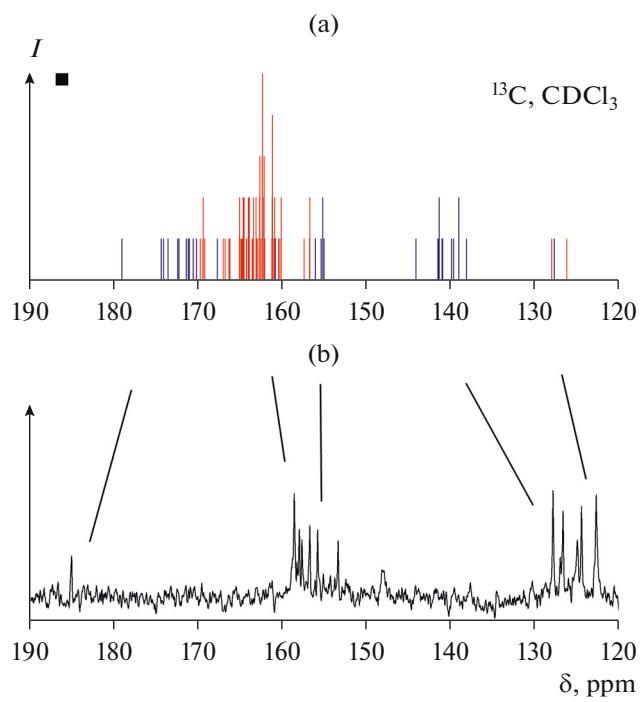


**Fig. 8.** Comparison of the (a) calculated and (b) experimental  $^{13}\text{C}$  NMR spectra for the product of the reaction of  $[\text{Mo}_3\text{S}_4\text{Cl}_3(\text{Dnbipy})_3]\text{PF}_6$  with  $\text{Pd}_2(\text{Dba})_3 \cdot \text{CHCl}_3$  and  $\text{C}_{60}$ . The signals from carbons of  $\text{C}_{60}$  are red-colored in the calculated spectrum, and the signals from the bipyridine ligand are blue-colored.

$[\text{Mo}_3\text{S}_4\text{Cl}_3(\text{Dnbipy})_3]\text{PF}_6$  with  $\text{Pd}_2(\text{Dba})_3 \cdot \text{CHCl}_3$  and  $\text{C}_{60}$  afforded a mixture of the products  $[\text{Mo}_3\text{Pd}(\text{C}_{60})\text{S}_4\text{Cl}_3(\text{R}_2\text{Bipy})_3]\text{PF}_6$  and  $\{[\text{Mo}_3\text{PdS}_4\text{Cl}_3(\text{R}_2\text{Bipy})_3]_2(\text{C}_{60})\}(\text{PF}_6)_2$ . Although no individual products were isolated, the coordination of fullerene to the palladium-containing cubane cluster was proved using the complex of spectroscopic methods and quantum-chemical calculations.

## FUNDING

This work was supported by the Russian Foundation for Basic Research, projects nos. 18-33-20056 and 19-33-90097.

## CONFLICT OF INTEREST

The authors declare that they have no conflicts of interest.

## REFERENCES

1. Krätschmer, W., Lamb, L.D., and Fostiropoulos, K.H.D.R., *Nature*, 1990, vol. 347, no. 6291, p. 354.
2. Moody, A., *Chem. Ind.*, 1991, p. 346.
3. Echegoyen, L. and Herranz, M.A., *Fullerenes: From Synthesis to Optoelectronic Properties*, Guidi, D.M. and Martin, N., Eds., Dordrecht: Springer, 2002.
4. Balch, A.L. and Olmstead, M.M., *Chem. Rev.*, 1998, vol. 98, no. 6, p. 2123.
5. Pan, Y., Liu, X., Zhang, W., et al., *Appl. Catal., B*, 2020, vol. 265, p. 118579.
6. Sulman, E., Matveeva, V., Semagina, N., et al., *J. Mol. Catal. A: Chem.*, 1999, vol. 146, nos. 1–2, p. 257.
7. Meng Ze-Da, Zhang Feng-Jun, Zhu Lei, et al., *Mater. Sci. Eng. C*, 2012, vol. 32, no. 8, p. 2175.
8. Signorini, R., Bozio, R., and Prato, M., *Fullerenes: From Synthesis to Optoelectronic Properties*, Guidi, D.M. and Martin, N., Eds., Dordrecht: Springer, 2002, p. 295.
9. Rispens, M.T. and Hummelen, J.C., *Fullerenes: From Synthesis to Optoelectronic Properties*, Guidi, D.M. and Martin, N., Eds., Dordrecht: Springer, 2002, vol. 60, p. 387.
10. Makarova, T., *Front. Magn. Mater.*, 2005, p. 209.
11. Johnston, H.J., Hutchison, G.R., Christensen, F.M., et al., *Toxicol. Sci.*, 2009, vol. 114, no. 2, p. 162.
12. Kausar, A., *Polym. Plast. Technol. Eng.*, 2017, vol. 56, no. 6, p. 594.
13. Konarev, D.V. and Lyubovskaya, R.N., *Russ. Chem. Rev.*, 2016, vol. 85, no. 11, p. 1215.
14. Megiatto, J.D., Guldi, D.M., and Schuster, D.I., *Chem. Soc. Rev.*, 2020, vol. 49, no. 1, p. 8.
15. Kleandrova, V.V., Luan, F., and Speck-Planche, A.C.M.N.D.S., *Curr. Bioinform.*, 2015, vol. 10, no. 5, p. 565.
16. Rašović, I., *Mater. Sci. Technol.*, 2017, vol. 33, no. 7, p. 777.

17. Espinet, P.A. and Albeniz, A.C., *Comprehensive Organomet. Chem. III*, 2007, no. 1995, p. 315.
18. Ohki, Y., Hara, R., Munakata, K., et al., *Inorg. Chem.*, 2019, vol. 58, no. 8, p. 5230.
19. Petrov, P.A. and Sukhikh, T.S., *Russ. J. Coord. Chem.*, 2019, vol. 45, no. 5, p. 333.  
<https://doi.org/10.1134/S1070328419040079>
20. Pedrajas, E., Sorribes, I., Guillamón, E., et al., *Chem. A Eur. J.*, 2017, vol. 23, no. 53, p. 13205.
21. Ohki, Y., Uchida, K., Hara, R., et al., *Chem. A Eur. J.*, 2018, vol. 24, no. 64, p. 17138.
22. Gushchin, A.L., Laricheva, Y.A., Sokolov, M.N., et al., *Russ. Chem. Rev.*, 2018, vol. 87, no. 7, p. 670.  
<https://doi.org/10.1070/RCR4800>
23. Oriwaki, K.M., Oshida, R.Y., and Kashi, H.A., *X-ray Struct. Anal. Online*, 2014, vol. 30, p. 11.
24. Gushchin, A.L., Sokolov, M.N., Naumov, D.Yu., and Fedin, V.P. *J. Struct. Chem.*, 2008, vol. 49, no. 4, p. 748.
25. Murata, T., Mizobe, Y., Gao, H., et al., *J. Am. Chem. Soc.*, 1994, vol. 116, no. 8, p. 3389.
26. Murata, T., Gao, H., Mizobe, Y., et al., *J. Am. Chem. Soc.*, 1992, vol. 114, no. 21, p. 8287.
27. Tao, Y., Zhou, Y., Qu, J., et al., *Tetrahedron Lett.*, 2010, vol. 51, no. 15, p. 1982.
28. Tao, Y., Wang, B., Wang, B., et al., *Org. Lett.*, 2010, vol. 12, no. 12, p. 2726.
29. Tao, Y., Wang, B., Zhao, J., et al., *Org. Chem.*, 2012, vol. 77, no. 6, p. 2942.
30. Wakabayashi, T., Ishii, Y., Ishikawa, K., et al., *Angew. Chem., Int. Ed. Engl.*, 1996, vol. 35, no. 18, p. 2123.
31. Sokolov, M.N., Chubarova, E.V., Virovets, A.V., et al., *J. Clust. Sci.*, 2003, vol. 14, no. 3, p. 227.
32. Sokolov, M.N., Virovets, A.V., Dybtsev, D.N., et al., *Communications*, 2001, no. 4, p. 4816.
33. Pino-Chamorro, J.A., Laricheva, Y.A., Guillamón, E., et al., *New J. Chem.*, 2016, vol. 40, no. 9, p. 7872.
34. Pedrajas, E., Sorribes, I., Gushchin, A.L., et al., *Chem-CatChem*, 2017, vol. 9, no. 6, p. 1128.
35. *ADF 2017. SCM, Theoretical Chemistry*, Amsterdam: Vrije Universiteit, 2017.
36. Frisch, M.J., Trucks, G.W., Schlegel, H.B., et al., *Gaussian I*, 2016.
37. Laricheva, Y.A., Gushchin, A.L., Abramov, P.A., et al., *Polyhedron*, 2018, vol. 154, p. 202.
38. Takei, I., Suzuki, K., Enta, Y., et al., *Organometallics*, 2003, vol. 22, no. 10, p. 1790.
39. Nagashima, H., Nakaoka, A., Saito, Y., et al., *Chem. Commun.*, 1992, no. 4, p. 377.
40. Basallote, M.G., Fernández-Trujillo, M.J., Pino-Chamorro, J.Á., et al., *Inorg. Chem.*, 2012, vol. 51, no. 12, p. 6794.
41. Algarra, A.G., Basallote, M.G., Fernandez-Trujillo, M.J., et al., *Inorg. Chem.*, 2010, vol. 49, no. 13, p. 5935.
42. Yanov, I., Leszczynski, J., Sulman, E., et al., *Int. J. Quantum Chem.*, 2004, vol. 100, no. 5, p. 810.
43. Brady, F.J., Cardina, D.J., and Domin, M., *J. Organomet. Chem.*, 1995, vol. 491, nos. 1–2, p. 169.

Translated by E. Yablonskaya